JOURNAL OF COMPUTATIONAL PHYSICS 67, 173–187 (1986)

An Application of the Random Choice Method to Reactive Gas with Many Chemical Species

YASUNARI TAKANO

Department of Applied Mathematics and Physics, Faculty of Engineering, Tottori University, Tottori, Japan

Received January 2, 1985; revised February 7, 1986

The random choice method is applied to one-dimensional problems for reactive gas with many chemical species. The random choice algorithm is extended to a multicomponent mixture. The extended random choice scheme is combined with a chemical kinetics simulation code to treat reactive gasdynamics. The method is used to calculate reflected-shock flowfields in H_2–O_2–Ar mixture and is shown to afford to describe complicated flowfields in detail. A comparison of the numerical results with shock-tube experiments shows good agreement. Also, a comparison between the random choice method and the FCT (Phoenical Lax–Wendroff) method as a solver of gasdynamics for multicomponent mixture indicates that they compute the reactive flows at the same profiles essentially and the former has better resolution for description of flowfields.

1. INTRODUCTION

The aim of this paper is to present an efficient and detailed computational tool to simulate one-dimensional gas flow in shock tubes, which have been intensively utilized to investigate chemical processes in real or combustible gas. Although the physical properties are constant behind shock waves in ideal gas, gasdynamic disturbances are produced by chemical reactions over the shocked regions in reactive gas. Therefore, for more precise determination of rate coefficients, it is important to perform simulations for comparison with experiments.

Oran, Young, and Boris [1] proposed a detailed modeling for shock and detonation phenomena by combining a finite difference scheme for gasdynamics with a chemical kinetics simulation code to describe fluid and chemical behaviors in reacting gas with many chemical species. The modeling was applied to simulate reflected-shock wave experiments in the weak and strong ignition regime in H_2–O_2–Ar mixture [2]. They used the flux corrected transport (FCT) method for gasdynamic calculations and the selected asymptotic integration (CHEMEQ) algorithm [4] for chemical simulation in their modeling.

Numerical procedures as a combination of gasdynamics and chemical kinetics can afford to provide useful tools to simulate shock tube experiments because they can reveal interaction between fluid motions and chemical processes which obscures

0021-9991/86 $3.00

chemical effect in experimental records. According to a review of finite difference methods for gasdynamics by Sod [5], the random choice method [6] has better advantages than conventional finite difference methods; it has generally higher resolution for flowfields, and produces no vibration behind shock waves and no smearing across contact discontinuities. We consider these advantages to be essentially suitable to simulations for reactive gasdynamics and hence apply the random choice method to reacting gas.

In the present investigation, the random choice algorithm deals with gasdynamic conservation equations which include species conservation as well as mass, momentum and energy conservation. It is combined with the selected asymptotic integration algorithm [4] to include chemical effects by using the operator splitting technique, by which Sod [7] applied the random choice method to cylindrically or spherically symmetric flow. As a numerical example of the present procedure, we calculate reflected-shock flowfield in H_2–O_2–Ar mixture and compare the results with pressure records of our shock-tube experiments. Also, a comparison is carried out between the random choice method and the FCT (Phoenical Lax–Wendroff) method [3] as a solver of gasdynamics for multi-component mixture.

It should be mentioned that Chorin [8] applied the random choice method to reactive gas flow. In his algorithm, detonation and deflagration are considered in addition to shock wave, expansion wave and contact discontinuity as solutions of Riemann problems for reactive gasdynamics, and chemical effect is treated briefly by introducing a progress parameter of chemical reactions. It can be said that this method, which was applied to problems for transition from deflagration to detonation [9], serves a different purpose from the present one which considers chemical effects accurately.

2. Numerical Model

2.1. *Basic Equations*

General forms of basic equations for reactive gas are described and explained by Oran and Boris [10]. The present investigation treats gasdynamic phenomena due to chemical reactions initiated by shock waves. As wave motions proceed much faster than transport processes in the present situations, the transport effects caused by viscosity, heat conduction and diffusion are neglected here.

The one-dimensional conservation equations for reactive gas with n components can be written as follows,

$$\frac{\partial U}{\partial t}+\frac{\partial F}{\partial x}=G, \tag{1}$$

$$\frac{\partial(\rho C)}{\partial t}+\frac{\partial(\rho u C)}{\partial x}=W, \tag{2}$$

$$p=\rho RT/M_w, \tag{3}$$

$$U=\begin{pmatrix}\rho\\ \rho u\\ p/(\gamma-1)+\frac{1}{2}\rho u^2\end{pmatrix},\qquad F=\begin{pmatrix}\rho u\\ \rho u^2+p\\ \{\gamma p/(\gamma-1)+\frac{1}{2}\rho u^2\}u\end{pmatrix},$$

$$G=\begin{pmatrix}0\\ 0\\ -\sum_{j=1}^{n} h_j^0\dot{\rho}_j\end{pmatrix},\qquad C=\begin{pmatrix}c_1\\ \vdots\\ c_n\end{pmatrix},\qquad W=\begin{pmatrix}\dot{\rho}_1\\ \vdots\\ \dot{\rho}_n\end{pmatrix}.$$

Here, ρ, u, p, T, γ, and M_w are the density, the velocity, the pressure, the temperature, the specific heat ratio, and the molecular weight of mixture, respectively. And, c_j, $\dot{\rho}_j$, and h_j^0 are the mass fraction, the rate of mass production and the enthalpy of formation for the jth species in the mixture. R is the universal gas constant.

For simplicity, we have assumed that the specific heat for each species remains constant as its dependence on the temperature is slight. Then, the enthalpy of the jth species reduces to

$$h_j=C_{pj}T+h_j^0,$$

where C_{pj} is its specific heat. Hence, we have the enthalpy of the mixture in the form as

$$h=C_pT+\sum_{j=1}^{n} c_jh_j^0,$$

where

$$C_p=\sum_{j=1}^{n} c_jC_{pj}.$$

In addition, the molecular weight and specific heat ratio for mixture can be expressed as, respectively,

$$M_w=\sum_{j=1}^{n}\frac{c_j}{M_j},\qquad \gamma=\frac{C_p}{C_p-R/M_w}.$$

As constant specific heat is assumed for each species, the specific heat ratio, γ, depends on the species concentrations but does not on the temperature, that simplifies algorithms of the random choice method for multicomponent mixture.

2.2. *Splitting Technique*

The splitting technique has been shown to be suitable to computations for reactive gas in which chemical reactions proceed much faster than fluid motions. Equations of reactive gasdynamics are split into terms due to fluid motions and due to chemical processes. The numerical integrations for chemical terms can be treated

separately by using an appropriate time step. Oran et al [1] simulated reactive shocks and Kee and Miller [11] calculated laminar diffusion flames by using the splitting technique. Also, Sod [7] employed the splitting technique to apply the random choice method to inhomogeneous equations for cylindrically or spherically symmetric flow.

When U^n and C^n, respectively, represent finite difference approximations to U and C at $t=n\Delta t$, the present computational schemes can be written as

$$\begin{pmatrix} U^{n+2} \\ C^{n+2} \end{pmatrix} = L_1(\Delta t)\, L_2(2\Delta t)\, L_1(\Delta t) \begin{pmatrix} U^n \\ C^n \end{pmatrix}, \tag{4}$$

for $n=0, 2, 4,\ldots$. Here, $L_1(\Delta t)$ is a finite difference operator which maps $U(t)$ and $C(t)$ into $U(t+\Delta t)$ and $C(t+\Delta t)$ using the following equations as

$$\frac{\partial U}{\partial t} + \frac{\partial F}{\partial x} = 0, \tag{5a}$$

$$\frac{\partial(\rho C)}{\partial t} + \frac{\partial(\rho u C)}{\partial x} = 0, \tag{5b}$$

and $L_2(\Delta t)$ also is a finite difference operator satisfying

$$\frac{\partial U}{\partial t} = G, \qquad \frac{\partial(\rho C)}{\partial t} = W. \tag{6ab}$$

Equations (5) represent gasdynamic behaviors without chemical reactions proceeding, while Eqs. (6) denote chemical behaviors in mixture under a constant volume condition. The numerical integration for Eqs. (6) are performed by choosing suitably fine time-steps as will be described.

We expect that a symmetrically split operator has better accuracy than asymmetric operators and employ the present scheme as shown in (4). Kee and Miller [11] discussed accuracy and efficiency for a symmetric operator of chemical steps sandwiched between transport steps as a numerical method for flame calculations.

2.3. *Fluid Motion*

As a solver for (5), we employ the random choice method which was introduced by Glimm [12] and has been developed by Chorin [6]. It is a semianalytical method which constructs approximate solution from exact solutions of Riemann problem by using a sampling procedure.

Solutions of the Riemann problem for ideal mixture are shown in Fig. 1 schematically. The initial data at $t=0$ is constant on each side of discontinuity at $x=0$, for example, ρ_L, u_L, p_L, c_{jL} for $x<0$ and ρ_R, u_R, p_R, c_{jR} for $x>0$. Here, c_j represents the mass fraction of the jth species which is a component of the vector C appearing in (2). The solution consists of four uniform regions with constant properties divided by right wave (RW) and left wave (LW), which are either a

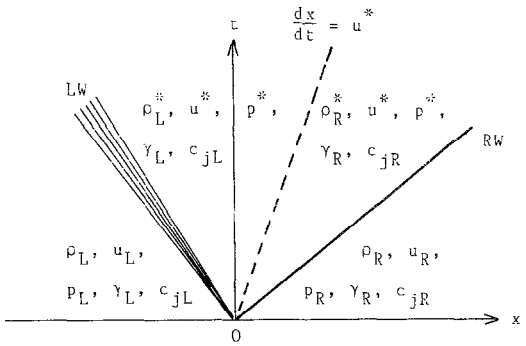

FIG. 1. Schematic diagram for solutions of Riemann problem.

shock wave or an expansion wave, and a slip line ($dx/dt = u^*$). In the present model, Riemann solutions for the physical properties ρ, u, and p are obtained through iterative algorithm which are extended to take account of variable specific heat ratio. See the Appendix. As is mentioned previously, the specific heat ratio does not depend on the temperature but on the species concentrations in the present framework. Hence, it is continuous across shocks and expansion wave but not always across the slip lines.

In addition to solutions of Eqs. (5a) for the properties, solutions of Eqs. (5b) for Riemann problems mentioned above can be written as follows

$$c_j(x, t) = \begin{cases} c_{j\mathrm{R}}, & x > u^* t \\ c_{j\mathrm{L}}, & x < u^* t. \end{cases} \tag{7}$$

These types of solutions are already described and discussed by Chorin [6] as a case that a passive quantity is transported by the fluid.

At every time-step, the approximate solution is piecewise constant on each intervals of length Δx; for example, it is constant in $(i-1/2)\,\Delta x < x < (i+1/2)\,\Delta x$ at $t = n\Delta t$ and also in $i\Delta x < x < (i+1)\,\Delta x$ at $t = (n+1)\,\Delta t$ as shown in Fig. 2, schematically. For $n\Delta t < t < (n+1)\,\Delta t$, an exact solution can be determined by

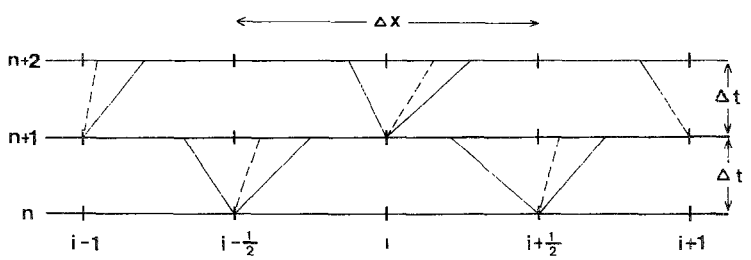

FIG. 2. Schematic diagram for grid points and approximate solution.

putting together solutions of Riemann problems in case waves originating from the points of discontinuity $x=(i+1/2)\,\Delta x$ do not interact each other. When $t\to(n+1)\,\Delta t$, the exact solution is not piecewise constant. The approximate solution at $t=(n+1)\,\Delta t$ is constructed so that the new constants in $i\Delta x<x<(i+1)\,\Delta x$, say $\rho'_{i+(1/2)}$, $u'_{i+(1/2)}$, $p'_{i+(1/2)}$, and $c'_{j,\,i+(1/2)}$, may be identical to the values of the exact solution on $x=(i+\theta_{n+1})\,\Delta x$ at $t=(n+1)\,\Delta t$ by using a sequence $\{\theta_n\}$ equidistributed on [0, 1]. At the time-step $t=(n+1)\,\Delta t$, chemical effects are considered on each interval as will be described in the following section. The pressure as well as the mass fractions are replaced from $p'_{i+(1/2)}$ and $c'_{j,\,i+(1/2)}$ to $p'_{i+(1/2)}+\Delta p_{i+(1/2)}$ and $c'_{j,\,i+(1/2)}+\Delta c_{j,\,i+(1/2)}$ satisfying Eqs. (6), while $\rho'_{i+(1/2)}$ and $u'_{i+(1/2)}$ are unchanged. After the effects of chemical reactions are taken into account, the random choice algorithm constructs an approximate solution at the time-step $t=(n+2)\,\Delta t$ from the Riemann data at $t=(n+1)\,\Delta t$.

We briefly mention how the random choice algorithm affords approximate solutions for the transport equations (5b). Consider an initial value problem where C (or c_j) is a step function at $t=0$. The solution for $t>0$ is a congruent step function propagating along a characteristic curve ($dx/dt=u$) originating from the discontinuity at $t=0$. An approximate solution by use of the random choice method is also a congruent step function staggering along the characteristic curve with a certain position error. As (5b) is a linear system by itself, approximations for general solutions are represented in combinations of staggering step functions in case initial data can be approximately expressed by superposing of step functions.

The random sampling procedure introduces position errors. Namely computed shock waves and contact discontinuities propagate staggering along their exact trajectories. These scatterings can be minimized by using rapidly equidistributed sequences. In the present computations, we employ the Van der Corput sampling sequences introduced by Colella [13].

In almost finite difference methods for gasdynamics, computations are carried out according to schemes which approximate differential equations by use of finite differences. When such convential finite difference methods are applied to (5b), the more time is necessary for computation, the more is the number of chemical species, because the computational time increases approximately proportional to the number of equations. On the contrary, for the random choice method, the computational time does not increase so much according to the number of chemical species. This is because the algorithm for the mass conservation equations (5b) consist of only samplings which need few processing time. Hence, the random choice method, which requires two or three time as much time to solve Eqs. (5a), becomes efficient compared with other method when it treats mixture with many chemical species.

2.4. *Chemical Processes*

Effects of chemical reactions are included in the modeling on the step of L_2 solving (6). From (6a), chemical reactions proceed on each mesh point under a

condition where the density and the velocity remain constant but the pressure varies due to release of chemical energy. Then, (6b) reduces to

$$\frac{\partial C}{\partial t} = \frac{1}{\rho} W(C, \rho, T). \tag{8}$$

For some interval between $i\Delta x$ and $(i+1)\Delta x$ at the time-step $t = (n+1)\Delta t$, the rate equations (8) are numerically integrated from the initial values of $c_j(t) = c'_{j,\, i+(1/2)}$ to $c_j(t+2\Delta t)$ with a constrained condition of $\rho = \rho'_{i+(1/2)}$. As a result of chemical proceedings on the step of $L_2(2\Delta t)$, the concentration of jth chemical species changes by

$$\Delta c_{j,\, i+(1/2)} = c_j(t+2\Delta t) - c_j(t),$$

and consequently, the pressure varies by

$$\Delta p_{i+(1/2)} = -(\gamma'_{i+(1/2)} - 1)\, \rho'_{i+(1/2)} \sum_{j=1}^{n} h_j^0 \Delta c_{j,\, i+(1/2)}.$$

We employ the selected asymptotic integration algorithm [4] for the numerical integration and refer to the general chemical kinetics computer program of Gordon and McBride [14] for the evaluation of $\dot{\rho}_j$ in W.

A step-size δt appropriate for the numerical integration of rate equations is chosen as $\delta t = 2\Delta t/l$ where l is a positive integer which is also stored on each interval (or mesh point) in addition to variables for the physical properties. The suitable step-size is decided according to criterions by Young and Boris [4]; when the algorithm does not converge iterated values to exact solutions within maximum iterations, five iterations for the present case, the time-step is reduced to be half as much, automatically; also when all convergences are achieved on the first iteration at an interval during the evaluation of $L_2(2\Delta t)$, the step-size on the interval at the next time-step starts from twice as much. It should be mentioned that there is a vectorized version of the selected asymptotic integration method available for users making use of vector processors [15].

2.5. *Appropriate Step-Sizes*

Although the random choice method treats shock waves and contact discontinuities as discontinuous profiles with perfect resolution, the random sampling procedure of the method introduces position errors which were estimated at $2.5\Delta x$ by Glimm, Marchesin, and McBryan [16]. Due to the randomness, physically smooth profiles may be computed at wrinkly profiles when a spacial step-size is not sufficiently small compared with a characteristic length of flowfields.

As numerical examples of the present method, simulations are made for reflected-shock waves in H_2-O_2–Ar mixture. For some conditions, compression waves generated by exothermic reactions are observed to develop to detonations as a

result of coupling of gasdynamics with chemical processes. In simulations for these detonation initiations, some oscillational errors are observed to superpose flowfields unless the spacial step-size is small enough to resolve steep profiles. When these oscillational errors appear over flowfields, step-sizes should be shortened to reduce the unphysical oscillations.

The ratio of time and spacial stepsizes must satisfy a CFL condition for the RCM:

$$\mathrm{Max}(|u|+a)\frac{\Delta t}{\Delta x}\leqslant\frac{1}{2},$$

where a $(=\sqrt{\gamma p/\rho})$ is the acoustic speed. We recommend use of a sufficiently small time-step for simulations of reactive gas with exothermic reactions because the fluid speed and the acoustic speed happen to increase due to chemical effects.

3. Discussions

3.1. *Numerical Examples*

Simulations are conducted for gasdynamic and chemical behaviors of reflected-shock waves in H_2–O_2–Ar mixture. Let x and t, respectively, be the distance from the end wall and the time after the shock reflection. Boundary conditions at the end wall can be written as follows

$$\rho(-x)=\rho(x), \qquad p(-x)=p(x), \qquad u(-x)=-u(x),$$
$$c_j(-x)=c_j(x) \qquad \text{for} \quad x>0.$$

In the simulations, we consider 13 elementary reactions with 8 chemical species such as Ar, H_2, O_2, H_2O, H, O, OH, HO_2 as shown in Table I, and employ the rate coefficient data given by Jensen and Jones [17].

The time and distance stepsizes are chosen as $\Delta t=0.0007\times t_{\mathrm{ind}}$ and $\Delta x=0.0014\times a_{\mathrm{f}}t_{\mathrm{ind}}$ where t_{ind} is the induction time of the mixture and a_{f} is the frozen acustic speed in the reflected-shock region. The Courant number for these step-sizes corresponds to 0.2–0.3 in the frozen reflected-shock region where chemical effects do not appear.

Computations were carried out by using FACOM M382 Computer at Data Processing Center in Kyoto University, which is comparable to IBM 370. A typical computational time is 15 min for the present examples which require 4000 time-steps over about 100 spacial meshes (or intervals) on an average.

3.2. *Results*

The results presented here are concerned with a phenomenon which happens after the reflection of an incident-shock wave at the speed of 0.725 km/sec moving into stationary mixture of 12 kPa Ar, 0.8 kPa H_2 and 0.4 kPa O_2 at 296° K. Figure 3 shows the x–t diagram of the reflected-shock flowfields.

TABLE 1

List of Chemical Reactions and Rate Coefficient Data

$k_r = A_r T^{n_r} \exp(-T_r/T)$				
r	Reactions	A_r	n_r	T_r
1	$H + O_2 = OH + O$	0.145E15[a]	0	8250
2	$O + H_2 = OH + H$	0.180E11	1	4480
3	$H_2 + OH = H_2O + H$	0.378E 9	1.3	1825
4	$O + H_2O = OH + OH$	0.590E14	0	9120
5	$H + HO_2 = OH + OH$	0.240E15	0	950
6	$OH + HO_2 = H_2O + O_2$	0.300E14	0	0
7	$O + HO_2 = OH + O_2$	0.480E14	0	500
8	$H + HO_2 = H_2 + O_2$	0.240E14	0	350
9	$H_2 + HO_2 = H_2O + OH$	0.600E12	0	9400
10	$H + O_2 + Ar = HO_2 + Ar$	0.160E16	0	−500
11	$H + H + Ar = H_2 + Ar$	0.110E19	−1	0
12	$O + O + Ar = O_2 + Ar$	0.725E17	−1	−200
13	$H + OH + Ar = H_2O + Ar$	0.360E23	−2	0

[a] $0.145E15 \equiv 0.145 \times 10^{15}$.

Figure 4 shows the pressure profiles which are plotted with a certain value shifted above at every 400 steps of computations. In the combustible mixture heated by reflected-shock wave, intermediate species such as H, O, and OH increase exponentially due to induction reactions which release almost no chemical energy. Therefore, no gasdynamic disturbance is generated in the reflected-shock flowfields

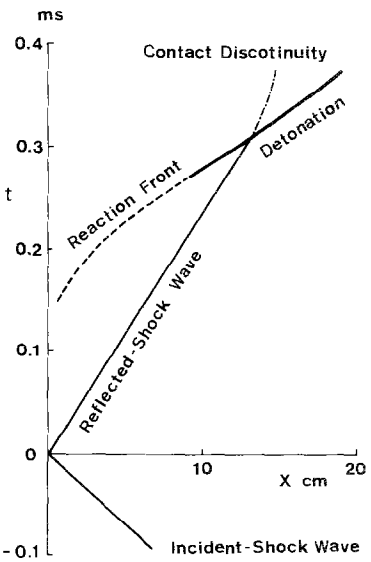

FIG. 3. X–t diagram for reflected-shock flowfields

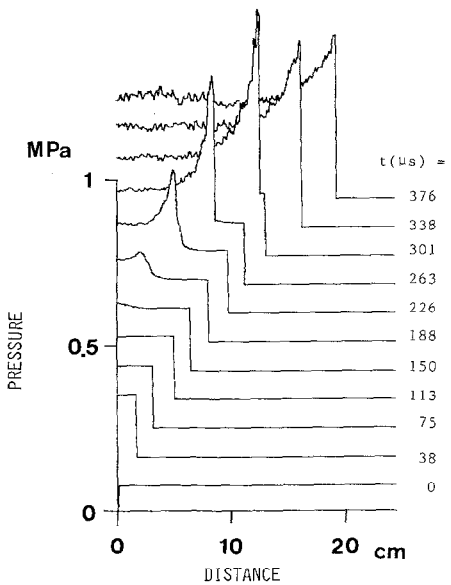

FIG. 4. Pressure profiles in the reflected-shock region.

for a while after the reflection. In the induction time, ignition takes place and compression waves propagate away from the end wall because of the heat release due to exothermic reactions.

Peaks of the concentration for OH in Fig. 5 correspond to ignition phase and also refer to the reaction front where the formation of H_2O and the heat release occurs rapidly. The OH concentration decays behind the reaction front due to

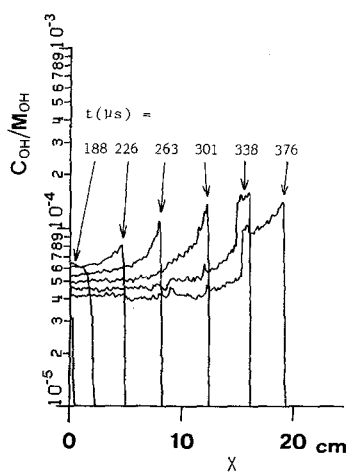

FIG. 5. Profiles of OH concentration in the reflected-shock region.

recombination reactions which release chemical heat considerably. Owing to the heat release, the temperature rises sharply behind the reaction front as shown in Fig. 6.

The reaction front is observed to accelerate as shown in Fig. 3. This is because the reduction of the induction time takes place due to slight temperature rises in front of the reaction front which are caused by compression waves. The accelerating reaction front produces stronger compression waves which develop to a shock wave. And consequently, the reaction front and the shock wave merge to a detonation wave which overtakes the reflected-shock wave.

3.3. *Comparison with Experiments*

The pressure histories on the end wall and on the side wall at the location ahead of the end wall by 54 mm are calculated to be compared with pressure records of our experiments. Takano and Akamatsu [18] reported our apparatus and its application to experiments for reactive gas.

Figure 7 shows comparisons between simulations and experiments for pressure records. In the end-wall pressure record, an increase of the pressure is generated due to heat release in the induction time after an abrupt pressure jump of shock reflection. On the other hand, a pressure pulse due to reaction front follows the pressure jumps due to incident- and reflected-shock waves. The comparisons of the simulation and the experiment are excellent with respect to the pressure records. Hence, it is shown that the present procedure can afford good simulations for shock-tube flows in reactive gas in case the flows are regarded as one-dimensional and essential reaction mechanisms are contained in the chemical model.

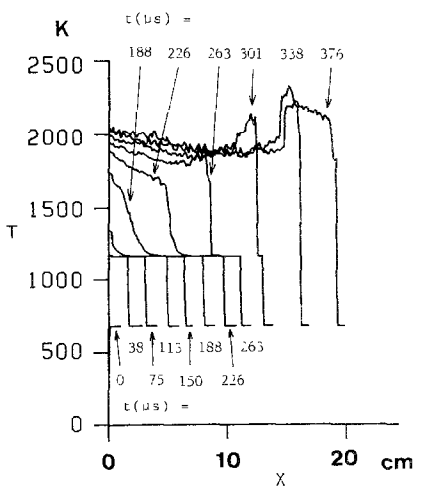

FIG. 6. Temperature profiles in the reflected-shock region.

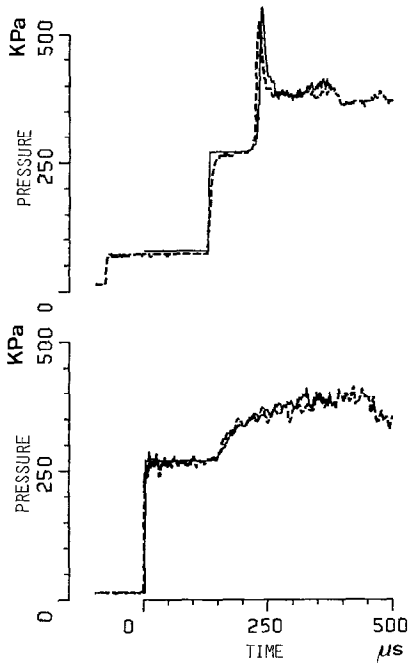

FIG. 7. Comparisons between simulation (—) and experiment (···) for the pressure records on the end wall (lower traces) and on the side wall (upper traces) of shock tube.

3.4. *Comparisons with the FCT Method*

To consider advantages and disadvantages of the present method in comparison with other methods, we choose the FCT (Phoenical Lax–Wendroff) method [3] as their representative because of its merits for calculations of gasdynamics with chemical reactions. It has been shown to produce no oscillations and has minimum artificial viscosity. Also, it has been already used for description of reactive gasdynamics [1, 2].

The results for the FCT version are shown in Figs. 8 and 9. Comparisons of the two methods for the density profiles in Fig. 8 show that they agree with each other quite well as shown at $t = 0.226$ ms. The RCM can afford to describe steep profiles for a detonation and a contact discontinuity generated from transmission of the detonation into the reflected-shock front as shown at $t = 0.376$ ms. In the results of the FCT version, it is observed that a peak of the detonation profile is blunted and a discontinuity of the contact surface is blurred. The RCM has such a disadvantage that it inherits to cause some vibrational errors due to random sampling. Comparisons for profiles of H atom concentration, shown in Fig. 9, indicate that chemical behaviors are somehow affected by physical behaviors.

In the present comparisons, the RCM version is shown to have better resolutions for flowfields with respect to steep detonation profiles and contact discontinuities.

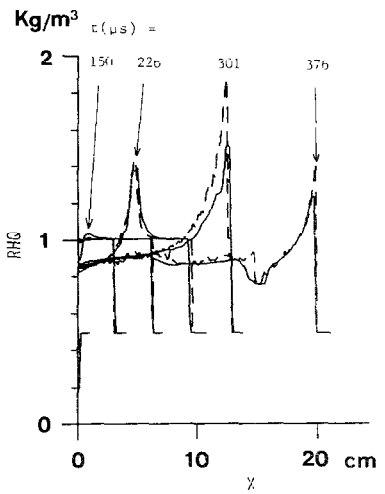

FIG. 8. Comparison between RCM (···) and FCT (—) for density profiles.

However, it should be mentioned that an adaptive gridding technique, which introduces fine grid points to locations of discontinuous profiles, is often used for the FCT method to obtain higher resolution.

3.5. *Applications*

It has been shown that the RCM is well applied to one-dimensional problems for reactive gasdynamics with many chemical species. The present method will be able to simulate shock-tube experiments for general combustible gas. Comparisons between experiments and simulations concerning with how compression waves caused by exothermic reactions accelerate the reactions will shed light on

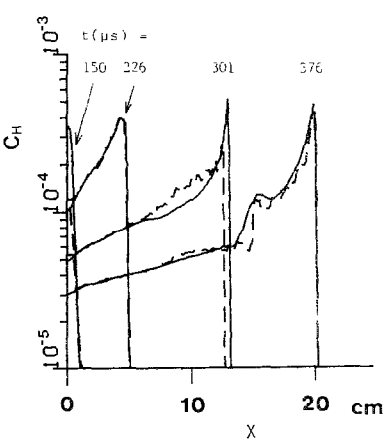

FIG. 9. Comparisons between RCM (···) and FCT (—) for profiles of H concentration.

mechanisms of exothermic reactions which are not so well understood as induction reactions.

The present method will not contribute to only experimental studies, but also to theoretical works. The present author employs the method to obtain exact solutions for reactive gasdynamics which are compared with results of a perturbation analysis [19]. Comparisons between the analysis and the simulations show an applicability of the analysis.

We will not apply the present method to two- and three-dimensional problems. Detailed simulations for multidimensional reactive flows are practically impossible due to computational time at present. Also, we feel it difficult to construct a multidimensional scheme from the present method by use of the operator splitting technique. This is because the multidimensional scheme of RCM was noted to produce large errors near a shock front [13].

4. Conclusions

In the present investigation, the random choice method is applied to one-dimensional problems of reactive mixture with many chemical species. It is performed by combining an extended random choice method to multicomponent gasdynamics with the chemical kinetics simulation code of the selected asymptotic integration algorithm. This procedure is applied to calculate reflected-shock waves in H_2–O_2–Ar mixture and has been shown to afford to describe reactive flowfields in detail. A comparison of the numerical results with pressure measurements of shock-tube experiments has indicated that the present method can simulate reactive flowfields in shock tubes in case flows can be treated one-dimensional and the chemical simulation modeling contains essential reaction mechanisms. A comparison of the present procedure with its FCT version, in which the gasdynamic solver is replaced by the FCT (Phoenical Lax–Wendroff) method, has indicated that they calculate reactive shock-flowfield at the same profiles essentially. Also, the method is observed to have higher resolution of flowfields.

Appendix: Extended Random-Choice Scheme to Multicomponent Gas

We explain extended parts of the random choice scheme, referring to the flowchart of RCM given by od [5]. In the part of Godunov interation to obtain p^* and u^*, shown in Fig. 1, which satisfy such relations as

$$M_R = (p_R - p^*)/(u_R - u^*),$$

$$M_L = (p_L - p^*)/(u_L - u^*),$$

where

$$M_R = (\rho_R p_R)^{1/2}\, \phi(p^*/p_R, \gamma_R),$$

$$M_L = (\rho_L p_L)^{1/2}\, \phi(p^*/p_L, \gamma_L),$$

we use

$$\phi(x,\gamma)=\left(\frac{\gamma+1}{2}x+\frac{\gamma-1}{2}\right)^{1/2}, \qquad x>1,$$

$$=\frac{\gamma-1}{2\gamma^{1/2}}\frac{1-x}{1-x^{(\gamma-1)/2\gamma}}, \qquad x<1.$$

It is notable that the function ϕ contains a variable γ for the specific heat ratio as well as a variable x for the ratio of the pressures.

In the part of the sampling due to Glimm, we use, respectively, γ_R or γ_L accordingly as the sampling point lies to the right or to the left of the slip line as shown in Fig. 1. In addition to the determination for the physical properties ρ, u, and p, the values for the mass fraction c_j are chosen c_{jR} or c_{jL} depending on whether the sampling point locates on the right or the left of the slip line.

ACKNOWLEDGMENTS

The author would like to express his appreciation to Professor T. Akamatsu of Kyoto University for his encouragments and Mr. S. Kittaka and Mr. S. Murata, respectively, former graduate student and undergraduate student of Kyoto University, for their conducting computations.

REFERENCES

1. E. S. ORAN, T. R. YOUNG, AND J. P. BORIS, *Seventeenth Symposium (International) on Combustion*, The Combustion Institute, 1978, p. 43.
2. E. S. ORAN, T. R. YOUNG, J. P. BORIS, AND A. COHEN, *Combust. Flame* **48**, 135 (1982).
3. D. L. BOOK, J. P. BORIS, AND K. HAIN, *J. Comput. Phys.* **18**, 248 (1975).
4. T. R. YOUNG AND J. P. BORIS, *J. Phys. Chem.* **81**, 2424 (1977).
5. G. A. SOD, *J. Comput. Phys.* **27**, 1 (1978).
6. A. J. CHORIN, *J. Comput. Phys.* **22**, 517 (1976).
7. G. A. SOD, *J. Fluid Mech.* **83**, 785 (1977).
8. A. J. CHORIN, *J. Comput. Phys.* **25**, 253 (1977).
9. Z. H. TENG, A. J. CHORIN, AND T. P. LIU, *SIAM J. Appl. Math.* **42**, 964 (1982).
10. E. S. ORAN AND J. P. BORIS, *Prog. Energy Combust. Sci.* **7**, 1 (1981).
11. R. J. KEE AND J. A. MILLER, *AIAA J.* **16**, 169 (1978).
12. J. GLIMM, *Comm. Pure Appl. Math.* **18**, 697 (1965).
13. P. COLELLA, *SIAM J. Stat. Comput.* **3**, 76 (1982).
14. S. GORDON AND B. J. MCBRIDE, NASA SP-273, 1976.
15. T. R. YOUNG, NRL Memo., Rep. No. 4091, 1980.
16. J. GLIMM, D. MARCHESIN AND O. MCBRYAN, *J. Comput. Phys.* **37**, 336 (1980).
17. D. E. JENSEN AND G. A. JONES, *Combust. Flame* **32**, 1 (1978).
18. Y. TAKANO AND T. AKAMATSU, *J. Phys. E: Sci. Instrum.* **17**, 644 (1984).
19. Y. TAKANO AND T. AKAMATSU, *J. Fluid Mech.* **160**, 29 (1985).